LETTERS

Neurosphere-derived multipotent precursors promote neuroprotection by an immunomodulatory mechanism

Stefano Pluchino[1], Lucia Zanotti[1], Barbara Rossi[3], Elena Brambilla[1], Linda Ottoboni[3], Giuliana Salani[1], Marianna Martinello[3], Alessandro Cattalini[1], Alessandra Bergami[1], Roberto Furlan[1,2], Giancarlo Comi[2], Gabriela Constantin[3] & Gianvito Martino[1,2]

In degenerative disorders of the central nervous system (CNS), transplantation of neural multipotent (stem) precursor cells (NPCs) is aimed at replacing damaged neural cells[1,2]. Here we show that in CNS inflammation, NPCs are able to promote neuroprotection by maintaining undifferentiated features and exerting unexpected immune-like functions. In a mouse model of chronic CNS inflammation, systemically injected adult syngeneic NPCs use constitutively activated integrins and functional chemokine receptors to selectively enter the inflamed CNS. These undifferentiated cells survive repeated episodes of CNS inflammation by accumulating within perivascular areas where reactive astrocytes, inflamed endothelial cells and encephalitogenic T cells produce neurogenic and gliogenic regulators. In perivascular CNS areas, surviving adult NPCs induce apoptosis of blood-borne CNS-infiltrating encephalitogenic T cells, thus protecting against chronic neural tissue loss as well as disease-related disability. These results indicate that undifferentiated adult NPCs have relevant therapeutic potential in chronic inflammatory CNS disorders because they display immune-like functions that promote long-lasting neuroprotection.

In CNS disorders characterized by chronic inflammation (for example, multiple sclerosis, brain tumours and ischaemic stroke), transplantation of NPCs might be expected to have little therapeutic effect, as recurrent or persisting inflammation may target and destroy both CNS-resident and transplanted cells. We assessed the therapeutic potential of subventricular-zone-derived syngenic adult NPCs (aNPCs) in a mouse model of chronic recurrent autoimmune CNS inflammation mimicking human multiple sclerosis—relapsing-remitting experimental autoimmune encephalomyelitis (R-EAE). As a long-term consequence of repeated inflammatory episodes, neurodegenerative features such as demyelination and axonal loss are present in mouse models of R-EAE[3].

SJL mice with R-EAE were injected intravenously with β-galactosidase (β-gal)-labelled aNPCs (1×10^6 cells per mouse) either at the first disease episode (13.1 ± 0.3 days post-immunization (dpi) with proteolipid protein (PLP)139–151) or at the occurrence of first clinical relapse (30.9 ± 1.1 dpi). Mice were observed for up to three months after transplantation. Clinical amelioration was observed using either treatment protocol (Table 1 and Supplementary Fig. 1). Mice transplanted with aNPCs at disease onset started to recover between 30 and 60 dpi, a period during which they underwent twofold fewer clinical relapses ($P \leq 0.05$) compared with sham-treated mice. A similarly low relapse rate was observed until the end of the follow-up period (106 dpi) ($P \leq 0.05$) compared with sham-treated mice. Mice transplanted with aNPCs at the onset of the first relapse started to recover later, but showed a threefold reduction in relapse rate between 60 and 90 dpi ($P \leq 0.005$ compared with sham-treated mice). At the end of the follow-up period, both treatment groups had a significantly lower R-EAE cumulative score and a significant reduction (58–80%) in the extent of demyelination and axonal loss compared with sham-treated mice.

Irrespective of whether aNPCs had been injected at R-EAE onset or at the first occurrence of clinical relapse, numerous β-gal-positive cells persisted within the CNS (Fig. 1 and Supplementary Fig. 2). No β-gal activity was found in the CNS of sham-treated mice (including in inflamed vessel walls) (Supplementary Fig. 2). At 106 dpi, we

Table 1 | Clinico-pathological features of R-EAE mice injected intravenously with aNPCs

Treatment	Treatment schedule	No. of mice	Disease onset (dpi)*	Maximum* clinical score	Cumulative disease score†	Relapse rate‡			Inflammatory infiltrates§ (number per mm^2)	Demyelination§ (% per mm^2)	Axonal loss§ (% per mm^2)
						0–30 dpi	30–60 dpi	60–90 dpi			
Sham	Disease onset	22	13.0 ± 0.2	2.6 ± 0.06	110.5 ± 8.1	1.4 ± 0.1	1.4 ± 0.1	1.2 ± 0.1	3.1 ± 0.5	1.4 ± 0.4	2.1 ± 0.4
aNPCs	Disease onset	13	13.1 ± 0.3	2.4 ± 0.1	64.5 ± 18.7¶	1.2 ± 0.1	0.7 ± 0.2‖	0.6 ± 0.2‖	2.04 ± 0.5	0.3 ± 0.08‖	0.6 ± 0.1‖
aNPCs	First relapse	13	14.5 ± 0.5	2.2 ± 0.08	45.6 ± 9.1#	1.8 ± 0.1	1.1 ± 0.1	0.4 ± 0.1¶	2.07 ± 0.4	0.6 ± 0.08‖	0.4 ± 0.07☆

*Data show mean number (±s.e.m.).
†The cumulative score (±s.e.m.) represents the sum of each individual score recorded for each mouse from the day of immunization (day 0) to the day on which the animal was killed (106 dpi).
‡The relapse rate represents the mean number of relapses (±s.e.m.) per mouse occurring in the indicated period.
§Inflammatory infiltrates, demyelination and axonal loss (mean ± s.e.m.) were quantified at time of death in an average of 12 spinal cord sections per mouse for a total of five mice per group.
‖$P \leq 0.05$ compared with sham-treated controls.
¶$P \leq 0.005$ compared with sham-treated controls.
#$P \leq 0.0005$ compared with sham-treated controls.
☆$P \leq 0.0001$ compared with sham-treated controls.

[1]Neuroimmunology Unit–DIBIT and [2]Department of Neurology and Neurophysiology, Vita-Salute University, San Raffaele Hospital, via Olgettina 58, 20132 Milano, Italy.
[3]Department of Pathology, Section of General Pathology, University of Verona, Strada le Grazie 8, 37134 Verona, Italy.

found 2.1 ± 0.2 β-gal-positive cells per mm^2 (mean ± s.e.m.) in mice transplanted with aNPCs at disease onset, and 4.1 ± 0.5 β-gal-positive cells per mm^2 in mice transplanted with aNPCs at first relapse. The great majority of β-gal-positive cells were located around inflamed deep blood vessels of the CNS, in close contact with blood-borne, CNS-infiltrating $CD45^+$ inflammatory immune cells (Fig. 1a, b), and maintained a round morphology typical of immature neural precursor cells (Fig. 1 and Supplementary Fig. 2). Some of the β-gal-positive cells showed positive staining for nestin (Fig. 1c, d; 0.28 ± 0.1 cells mm^{-2}), neuron-specific nuclear protein (NeuN) (Fig. 1e, f; 0.21 ± 0.1 cells mm^{-2}) or distal-less-related (Dlx)-2 (Fig. 1h, i; 0.12 ± 0.1 cells mm^{-2}), and a few were immunoreactive for the proneural transcription factor mammalian achaete-scute homologue (Mash)-1 (ref. 4, Fig. 1g) or for polysialylated neural cell adhesion molecule (PSA-NCAM)[5] (Fig. 1j–m). None of the β-gal-positive cells showed immunoreactivity for NG2, glial fibrillary acidic protein (GFAP) (Supplementary Fig. 3), β-tubulin III or platelet-derived growth factor (PDGF) receptor-α. Occasionally, transplanted aNPCs showing a stream-like tubular pattern of chain migration—reminiscent of that described for migrating neuroblasts within stem cell niches of the adult brain[6,7]—were found in close contact with the blood vessel wall (Supplementary Fig. 2).

To better define the proliferation dynamics of aNPCs persisting within the CNS, R-EAE mice were treated with 5-bromodeoxyuridine (BrdU) at 106 dpi. A consistent fraction of transplanted β-gal-positive cells were BrdU-positive: 7.3 ± 1.5% in mice receiving aNPC transplants at disease onset, and 8.4 ± 1.4% in mice transplanted with aNPCs at first relapse (Fig. 1n). Occasionally, $\beta\text{-gal}^+BrdU^+$ cells expressed early differentiation markers (for example, PSA-NCAM) (Supplementary Fig. 3). A long-term study of neural stem/progenitor cell marker and BrdU labelling to prove the similarity between perivascular CNS areas in R-EAE mouse models and stem cell niches in adult brain is still lacking. However, our description of a subpopulation of intravenously injected cells that proliferate and maintain an (early) differentiated phenotype around blood vessels indicates that inflamed CNS perivascular areas in R-EAE might function as ideal, but atypical, niche-like areas in which transplanted cells can survive for a long time (up to three months after transplantation) as bona fide aNPCs.

We then turned to putative mechanism(s) that might favour aNPC

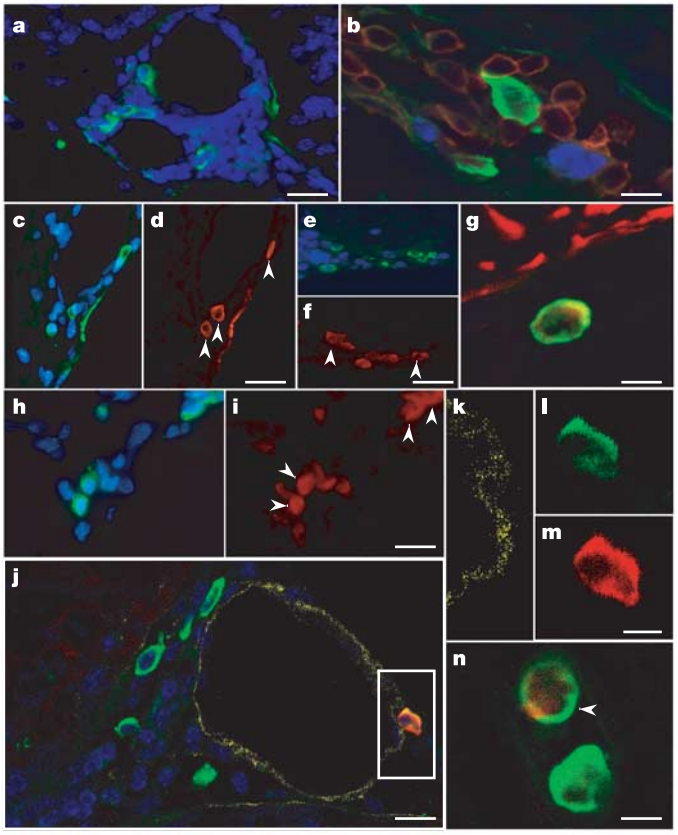

Figure 1 | aNPCs transplanted intravenously persist in inflamed perivascular areas of the CNS for up to three months after transplantation in R-EAE mice. **a**, **b**, β-gal-labelled, intravenously injected aNPCs (green) remain in perivascular CNS areas where blood-borne $CD45^+$ immune cells (red in **b**) that form the CNS inflammatory infiltrate persist. $CD45^+$ cells within perivascular areas are Ki67-negative, indicating that they are final effector encephalitogenic cells. Nuclei in **a** are in blue (DAPI). Ki67-positive cells in **b** are stained blue. **c**–**m**, Within perivascular areas, some of the β-gal-labelled cells (green in **c**, **e**, **g**, **h**, **j**, **l**) are positive for nestin (red, arrowheads in **d**), NeuN (red, arrowheads in **f**), Mash-I (red in **g**), Dlx-2 (red, arrowheads in **i**) and PSA-NCAM (red in **j**, **m**). In **j** and **k**, CNS blood vessels are stained with laminin (yellow). The inset in **j** is shown in **k**–**m**. Nuclei in **c**, **e**, **h** and **j** are in blue (DAPI). **n**, A β-gal-labelled, intravenously injected aNPC (green) stained for BrdU (red, arrowhead). Scale bars, 10 μm (**m**, **n**), 15 μm (**b**, **g**), 20 μm (**j**), 25 μm (**f**), 30 μm (**a**, **d**), 40 μm (**i**).

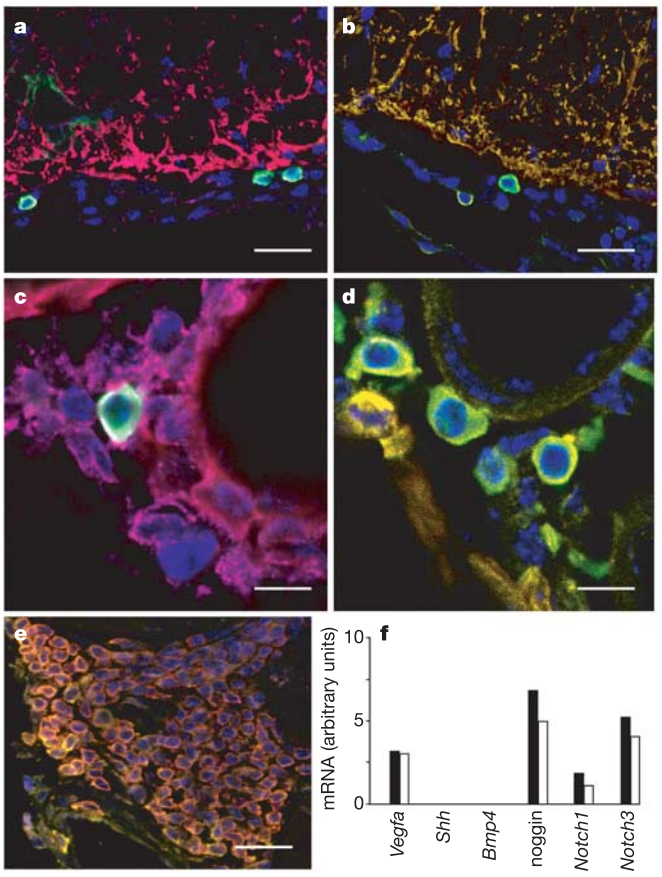

Figure 2 | Stem cell regulators co-localize with intravenously injected aNPCs that persist in perivascular areas of the CNS in R-EAE mice. **a**–**d**, In perivascular CNS areas, GFAP-positive astrocytes (red in **a**, **b**) and laminin-positive endothelial cells (red in **c**, **d**) that secrete BMP-4 (magenta in **a**, **c**) and noggin (yellow in **b**, **d**) co-localize with transplanted β-gal-positive aNPCs (green in **a**–**d**). **e**, Perivascular CNS area containing infiltrating final effector $CD45^+$ lymphocytes (red) secreting noggin (yellow). Nuclei are in blue (DAPI). See Supplementary Fig. 5 for images of single staining. Scale bars, 40 μm (**a**, **b**), 25 μm (**c**, **d**), 50 μm (**e**). **f**, Real-time PCR showing mRNA levels of stem cell regulators in spleen-derived lymphocytes from naive SJL mice. Both concanavalin (Con)A-activated (black bars) and resting lymphocytes (white bars) produce *Vegfa*, noggin, *Notch1* and *Notch3* mRNA.

survival in inflamed perivascular CNS areas. Irrespective of aNPC transplantation, protein expression of stem cell regulators and growth factors involved both in angiogenesis and neurogenesis (for example, bone morphogenetic proteins (BMPs), noggin, notch-1, jagged-1 and vascular endothelial growth factor (VEGF)-α)[8,9] were found in these areas until 106 dpi (Supplementary Fig. 4). BMP-4 and noggin (Fig. 2 and Supplementary Fig. 5) were secreted not only by β-gal$^-$GFAP$^+$ astrocytes (Fig. 2a, b) and β-gal$^-$laminin$^+$ endothelial cells (Fig. 2c, d), but also by blood-borne CNS-infiltrating CD45$^+$ inflammatory cells (Fig. 2e). This latter result was confirmed at the messenger RNA level in spleen-derived lymphocytes (Fig. 2f).

We also investigated the cellular and molecular basis by which intravenously injected aNPCs selectively reached inflamed perivascular CNS areas in R-EAE mice. Irrespective of the mouse strain (C57BL/6 or SJL), we found that half (53 ± 10%) of aNPCs express the α4 subunit of the integrin very late antigen (VLA)-4 as a constitutively activated molecule organized in clusters (12 ± 5% cells were negative for VLA-4 and 31 ± 9% had a 'dispersed' distribution; Fig. 3a, b), a finding similar to that described in immune cells[10]. Spontaneous adhesion of aNPCs to purified vascular cell adhesion molecule (VCAM)-1—the VLA-4 counterligand—was basally high and comparable to that obtained with mitogen-activated CD4$^+$ cells (Fig. 3c). This adhesion was not significantly increased after stimulation with chemokines such as CCL2/MCP-1, CXCL9/MIG, CXCL10/IP-10, CXCL11/I-TAC, and CXCL12/SDF-1α (Fig. 3c). The ability of aNPCs to spontaneously adhere to VCAM-1-expressing cells was confirmed using intravital microscopy in a subacute C57BL/6 mouse model of brain inflammation, in which upregulation of VCAM-1 expression on microvessels was obtained by intraperitoneal injection of lipopolysaccharide (LPS)[11] (Fig. 3d). This finding was further supported by the specific binding of aNPCs to venules from pectoral muscle ectopically overexpressing VCAM-1 (Fig. 3e–g). A monoclonal antibody against VCAM-1 blocked more than 60% of stable aNPC adhesion (both in brain and muscle), but isotype-matched, anti-ICAM-1 and anti-MAdCAM-1 antibodies had no significant effect (data not shown).

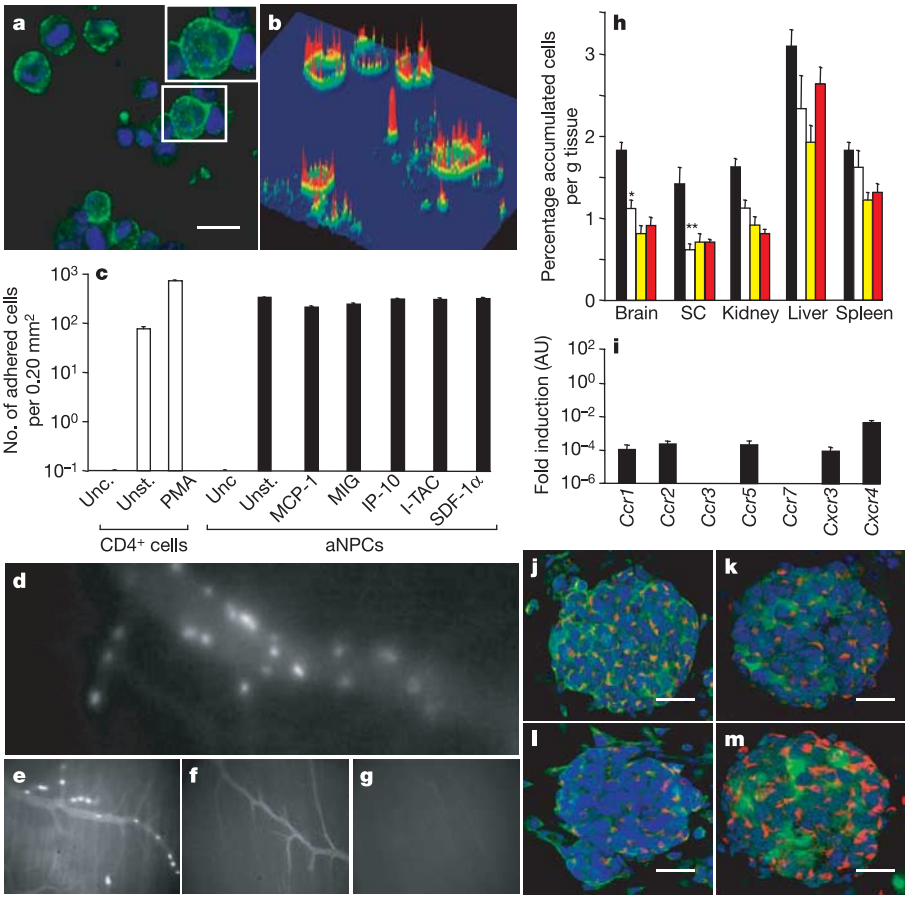

Figure 3 | aNPCs constitutively expressing VLA-4 and chemokine receptors accumulate around inflamed CNS microvessels in R-EAE mice. **a**, **b**, Clustering (**a**, green) and 3-dimensional plot of fluorescence intensity (**b**) of VLA-4 on aNPCs. Nuclei are shown in blue (DAPI). Scale bar, 20 μm. **c**, Unstimulated (Unst.) aNPCs and PMA-stimulated CD4$^+$ T cells adhere to VCAM-1 *in vitro*. Binding does not increase when aNPCs are stimulated (for 3 min at 37 °C) with different chemokines at 1 μM. Adhesion is completely absent in uncoated (Unc.) wells. Results expressed as mean number (±s.e.m.) of adherent cells per 0.2 mm^2. **d**, **e**, Intravital microscopy showing aNPCs (bright intravascular dots) firmly adhering to inflamed brain (**d**) and striate muscle venules (**e**) from LPS-treated mice (×20 original magnification). **f**, **g**, VCAM-1 expression in inflamed striate muscle venules (**f**); isotype-matched control antibody (anti-human Ras) is shown in **g**. **h**, Accumulation of 2,3-[^{3}H]-glycerol-labelled aNPCs in different organs from R-EAE (black bars) and naive control (yellow bars) mice 24 h after intravenous injection. An anti-VLA-4 antibody decreases aNPC recruitment in the brain (39%) and spinal cord (SC, 54%) in R-EAE (white bars) but not in naive control mice (red bars). Asterisk, $P = 0.005$; two asterisks, $P \leq 0.0001$. Results expressed as mean percentage (±s.e.m.) of accumulated cells per gram of tissue from four independent experiments. **i**, Mouse aNPCs express detectable levels of chemokine receptor *Ccr1*, *Ccr2*, *Ccr5*, *Cxcr3* and *Cxcr4* mRNA, but not *Ccr3* and *Ccr7* mRNA. Results are the mean of three independent experiments and show fold induction (mean ± s.d.) of mRNA levels detected in aNPCs over ConA-activated splenocytes, which were used as a positive internal control. **j**–**m**, Nestin-positive aNPCs (red) express CCR2 (**j**), CCR5 (**k**), CXCR3 (**l**) and CXCR4 (**m**). Receptors are stained in green in their respective panels, nuclei are in blue (DAPI). Scale bars, 80 μm (**j**–**l**), 120 μm (**m**).

To verify the relevance of this phenomenon in R-EAE mice, ^{3}H-glycerol-labelled aNPCs (2×10^{6} cells per mouse) were injected intravenously into proteolipid protein (PLP)139–151-immunized SJL mice at the time of the first disease episode. Within 24 h of cell injection, aNPCs were found in various bodily organs, and $3.1 \pm 0.2\%$ of the cells had accumulated in the CNS (Fig. 3h). A significant reduction in aNPC recruitment to the CNS (39–54% reduction; $P \leq 0.005$) was observed after *in vitro* pre-treatment of aNPCs with an anti-VLA-4 blocking antibody (Fig. 3h). This effect was EAE-specific, as VLA-4 blocking did not result in decreased cell recruitment into the CNS (and other peripheral organs) of naive mice injected intravenously with labelled aNPCs (Fig. 3h). These results were also confirmed in a chronic progressive model of EAE in C57BL/6 mice (Supplementary Fig. 6).

Our *in vitro* studies showed that pro-inflammatory chemokines do not further activate basal avidity for counterligands of VLA-4 expressed on aNPCs (Fig. 3c). However, we cannot exclude the possibility that culturing cells with mitogens might somehow influence VLA-4 basal avidity on aNPCs *in vitro*. G-protein-coupled receptors (GPCRs) might be necessary for further increasing aNPC transendothelial migration or for mediating environmental positioning under suboptimal conditions, such as those that might occur *in vivo*[12,13]. We found that aNPCs express a wide range of pro-inflammatory chemokine receptors, at both mRNA and protein levels. Most cells within neurospheres express the chemokine receptors CCR1, CCR2, CCR5, CXCR3 and CXCR4, but do not express CCR3 or CCR7 (Fig. 3i–m). CCR1, CCR5 and CXCR4 were functionally active, as aNPCs migrated in a dose-dependent manner in response to the chemokines CCL5/RANTES and CXCL12/SDF-1α (Supplementary Fig. 7). Pre-treatment of aNPCs with the G_i-protein inhibitor pertussis toxin completely inhibited this migration response, showing that it was GPCR-dependent (Supplementary Fig. 7). Thus, aNPCs might use GPCRs and cell adhesion molecules to increase their migration towards inflamed lesions in the CNS. This explains the partial inhibition of aNPCs extravasation obtained in R-EAE mice using an anti-α4-integrin blocking antibody.

We propose that inflammation acts as the 'danger signal' that determines both selective recruitment and long-term survival of intravenously injected aNPCs in the CNS of R-EAE mice. However, the mechanism(s) by which transplanted aNPCs act to protect mice from R-EAE remains to be identified. Apoptosis is considered one of the principal mechanisms for promoting recovery from EAE, by inducing programmed cell death of CNS-infiltrating encephalitogenic T cells[14,15]. As early as two weeks after aNPC transplantation (30 dpi), R-EAE mice receiving transplants at disease onset showed a significant reduction in the number of inflammatory infiltrates in the CNS ($P \leq 0.01$) and a threefold increase in the number of CNS-infiltrating $CD3^{+}TUNEL^{+}$ cells ($P \leq 0.005$ compared with sham-treated mice) (Fig. 4a and Supplementary Fig. 8). In both aNPC- and sham-treated mice, the majority ($83.8 \pm 6.9\%$ and $90.5 \pm 2.3\%$, respectively) of apoptotic cells were confined to CNS perivascular inflammatory infiltrates. These results were confirmed using active caspase-3 as a marker for apoptosis, and also showed that transplanted β-gal-positive cells in inflamed perivascular CNS areas did not undergo apoptosis (Fig. 4b). At 50 dpi, fluorescence-activated cell sorting (FACS) analysis of CNS-infiltrating $CD3^{+}$

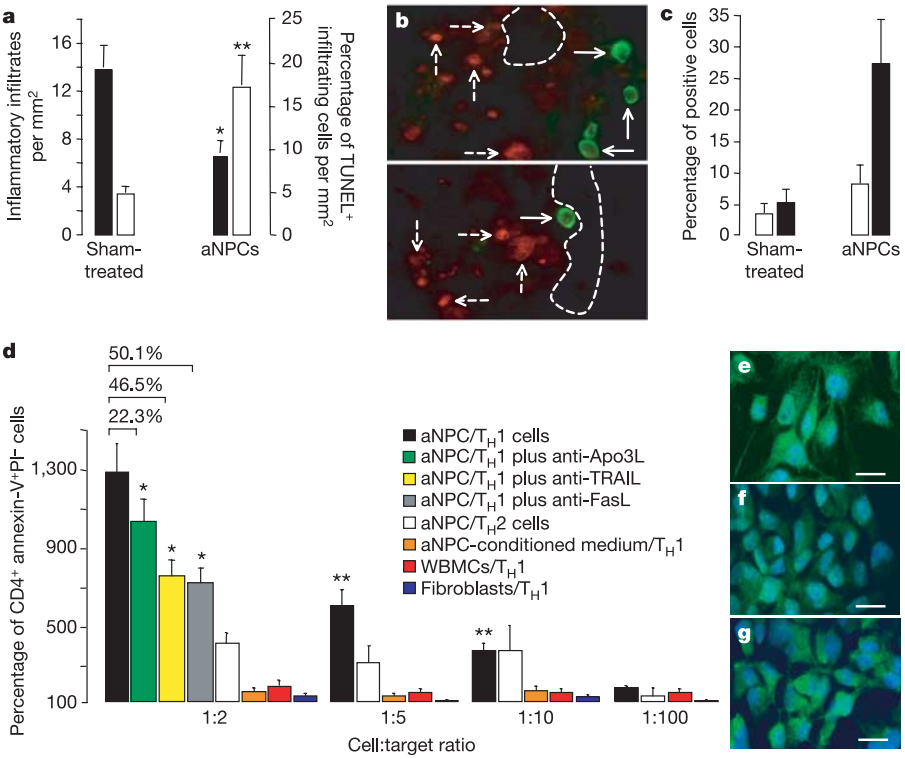

Figure 4 | aNPCs induce apoptosis of encephalitogenic T cells *in vitro* and *in vivo*. **a**, Decrease in spinal cord inflammation (black bars) and increase in CNS-infiltrating apoptotic lymphocytes (white bars) in R-EAE mice 15 days after aNPC injection (30 dpi) (mean ± s.e.m.). Asterisk, $P \leq 0.01$; two asterisks, $P \leq 0.005$ compared with sham-treated mice. **b**, Spinal cord perivascular area stained for caspase-3 (red, dashed arrows) and β-gal (green, solid arrows). Dashed lines indicate blood vessels (× 100 original magnification). **c**, FACS analysis showing a significant increase in late apoptotic ($TOPRO3^{+}AnnexinV^{+}$, black bars) but not necrotic ($TOPRO3^{+}AnnexinV^{-}$, white bars) CNS-infiltrating $CD3^{+}$ T cells in R-EAE mice 35 days after aNPC injection (50 dpi). Results expressed as mean percentage of positive cells (±s.e.m.) from three independent experiments. **d**, aNPCs induce apoptosis ($AnnexinV^{+}PI^{-}$ cells) of PLP139–151-specific T_H1 but not T_H2 cell lines (two asterisks, $P \leq 0.05$ versus basal levels). Inhibition of FasL, Apo3L or TRAIL significantly reduces the aNPC-mediated pro-apoptotic effect (asterisk, $P \leq 0.01$). Results (mean ± s.e.m.) from three independent experiments. **e**–**g**, Fluorescence images showing expression of death receptors FasL/CD95-ligand (**e**), Apo3L (**f**) and TRAIL (**g**) on aNPCs conditioned with pro-inflammatory cytokines. Nuclei are in blue (DAPI). Scale bars, 15 μm.

cells showed a significantly ($P = 0.01$) higher percentage (27.3 ± 10.4%) of annexin-V$^+$TOPRO-3$^+$ 'late apoptotic' cells in R-EAE mice transplanted at onset compared with sham-treated mice (5.2 ± 0.6%) (Fig. 4c).

In the same mice, CNS-infiltrating CD3$^+$ cells did not show any sign of immunological anergy, as indicated by non-significant differences in the percentages of cells producing interferon (IFN)-γ (17.6 ± 2.26% sham-treated versus 12.2 ± 3.53% aNPC-treated) or interleukin (IL)-2 (17.8 ± 1.64% versus 33.6 ± 10.7%), or those producing both IFN-γ and IL-2 (59.3 ± 1.96% versus 41.0 ± 15.7%). The pro-apoptotic effect of aNPCs on T cells was also confirmed by *in vitro* analyses. Spleen-derived CD3$^+$ cells from naive syngenic SJL mice that had been activated by plastic-immobilized anti-CD3/CD28 antibody underwent apoptosis when co-cultured with increasing numbers of single-cell dissociated aNPCs. In a transwell system designed to prevent cell-to-cell contact, the pro-apoptotic effect of aNPCs on CD3$^+$ cells was less intense but still measurable (Supplementary Fig. 8). Furthermore, *in vitro* generated antigen (PLP139–151 peptide)-specific CD4$^+$ T-cell lines with a pro-inflammatory type 1 helper (T_H1) cytokine profile (for example, secreting tumour necrosis factor (TNF)-α and interferon (IFN)-γ), but not PLP139–151-specific CD4$^+$ T-cell lines with an anti-inflammatory T_H2 cytokine profile (for example, secreting IL-4), underwent apoptosis when co-cultured *in vitro* with increasing numbers of single-cell dissociated aNPCs (Fig. 4d). However, fibroblasts, whole bone marrow cells or aNPC-conditioned medium did not induce measurable pro-apoptotic effects when co-cultured with PLP139–151-specific T_H1 cells.

In vitro and *in vivo* data suggest that aNPC-mediated apoptosis might be induced through both (extrinsic) death receptor- and (intrinsic) mitochondrial-mediated pathways (see ref. 16 for a review). Blockade of death receptor ligands, but not of IFN-γ and inducible nitric oxide synthase (iNOS), significantly decreased apoptosis of PLP139–151-specific T_H1 cells (22.3–50.1%; Fig. 4d), indicating involvement predominantly of the death receptor pathway. However, we still cannot exclude involvement of the mitochondrial apoptotic pathway. In fact, aNPCs conditioned *in vitro* with pro-inflammatory cytokines (such as TNF-α, IFN-γ and IL-1β)[17] greatly increased (at both protein and mRNA levels) not only the membrane expression of death receptor ligands (for example, FasL, Trail and Apo3L) (Fig. 4e–g) but also the production of soluble factors potentially involved in mitochondrial-mediated apoptosis, including iNOS, IFN-γ, glial-derived neurotrophic factor (GDNF) and leukaemia inhibitory factor (LIF)[15,16,18,19] (Supplementary Figs 8 and 9). Thus, our results indicate that aNPC-mediated T-cell apoptosis can occur via multiple distinct pathways, with the death receptor-mediated pathway probably the predominant one.

Finally, at 106 dpi we found increased numbers of process-bearing CD11b$^+$ activated microglial cells within perivascular CNS areas from aNPC-treated R-EAE mice (79.7 ± 10.8 cells mm^{-2} in mice treated at onset, 58.6 ± 5.6 cells mm^{-2} in mice treated at first relapse, 3.3 ± 0.8 cells mm^{-2} in sham-treated mice, $P < 0.001$; Supplementary Fig. 4). These microglial cells were found capable of producing pro-apoptotic substances upon *in vitro* activation with pro-inflammatory cytokines (Supplementary Fig. 8). We must therefore consider the possibility that CNS-resident glial cells might also contribute to promote T-cell apoptosis, as previously suggested[20].

Here we demonstrate that undifferentiated aNPCs can promote brain repair upon systemic injection into a mouse model of multiple sclerosis through previously unidentified immune-like functions. This observation is consistent with earlier reports indicating that transplanted aNPCs promote brain repair as they acquire a terminally differentiated phenotype *in vivo*[2,21]. Our data indicate that the CNS microenvironment dictates the fate (and consequently, the therapeutic efficacy) of systemically transplanted aNPCs. When neurodegeneration prevails, transplanted cells acquire a mature functional phenotype and thus replace damaged neural cells[2,21,22]. As we show here, when neuroinflammation predominates, transplanted aNPCs survive recurrent inflammatory episodes by retaining both an undifferentiated phenotype and the ability to proliferate. In this situation, inflammation represents the key danger signal for orchestrating recruitment to and long-term persistence of aNPCs in areas of CNS damage. Recruitment is possible because of the innate capacity of circulating aNPCs to use selected molecular pathways (for example, integrin- and chemokine-mediated homing) used by blood-borne-derived lymphocytes in patrolling the CNS. Long-lasting persistence of aNPCs in the CNS is due to continuous cross-talk between transplanted aNPCs and inflammatory CNS-infiltrating T cells within perivascular niche-like areas, together with CNS-resident cells that produce gliogenic and neurogenic regulators. In these areas, aNPCs survive as undifferentiated cells and exert neuroprotective effects by inducing programmed cell death of blood-borne, CNS-infiltrating pro-inflammatory T_H1 (but not anti-inflammatory T_H2) cells[23,24].

METHODS

Adult NPC derivation and cultures. Cultures of adult NPCs were established from the subventricular zone of brains from 6–8-week-old SJL and C57BL/6 mice, as previously described[2]. Details are provided in the Supplementary Methods.

R-EAE induction. SJL mice (Charles-River) were immunized with 200 μg PLP139–151 (Espikem) in complete Freund's adjuvant (CFA) as described[3]. Body weight and clinical score (0 = healthy; 1 = limp tail; 2 = ataxia and/or paresis of hind limbs; 3 = paralysis of hind limbs and/or paresis of forelimbs; 4 = tetra paralysis; 5 = moribund or dead) were recorded daily. Clinical relapses were defined as the occurrence of an increase in clinical score of 0.5 persisting for a minimum of three consecutive days.

aNPC cell transplantation. β-gal-positive aNPCs were injected intravenously through the tail vein[2]. Sham-treated age-, sex- and strain-matched mice injected intravenously with PBS alone were used as controls. To assess the *in situ* proliferation of intravenously injected aNPCs, mice were treated intraperitoneally with bromodeoxyuridine (BrdU, Roche, 50 mg kg^{-1}) at 106 dpi for three consecutive days and killed soon thereafter, as previously described[25]. Details are provided in the Supplementary Methods.

Neuropathology. The brain and spinal cord of mice were removed and processed for pathology. Either paraffin-embedded or frozen tissue samples were used. Detailed descriptions of procedures and the list of antibodies are provided in the Supplementary Methods.

Immunocytochemistry. Single-cell dissociated or sphere-aggregated aNPCs were plated at 3×10^4 cells cm^{-2} onto matrigel-coated glass chamber slides in growth medium and incubated for 1 h at 37 °C. Fluorescent samples were analysed using a BioRad MRC 1024 confocal image microscope. Image Pro plus software was used for VLA-4 distribution analysis. The complete list of antibodies is provided in the Supplementary Methods.

***In vivo* distribution of aNPCs.** aNPCs (2×10^6 cells per mouse) were incubated for 4 h at 37 °C in growth medium containing 100 μCi ml^{-1} 2,3-[3H]glycerol (MP Biomedicals) and then injected intravenously into (1) C57BL/6 mice that had been immunized with 200 μg myelin oligodendrocyte glycoprotein (MOG)35–55 (Espikem) in CFA containing 500 ng pertussis toxin[2] or (2) SJL mice that had been immunized with PLP139–151 (ref. 3). Mice were injected soon after disease onset and killed 24 h after transplantation. After perfusion, brain, spinal cord, kidney, spleen and liver were collected, weighed and sonicated, and the radioactive content of the tissues measured in a β-counter (LS1801; Beckman Coulter) as previously described[26]. Data are expressed as mean percentage (±s.e.m.) of accumulated cells per gram of tissue from a minimum of six mice per group from four independent experiments.

Static adhesion assay. aNPCs were added to 18-well glass slides at 7×10^4 cells per well in 25 μl, and coated overnight at 4 °C with (1 μg ml^{-1}) purified mouse VCAM-1 (RAND D, gift from E. Butcher) as previously described[10]. Spleen-derived CD4$^+$ T cells (7×10^4 cells per well in 25 μl) stimulated for 10 min with the mitogen phorbol 12-myristate 13-acetate (PMA, 100 ng ml^{-1}) were used as positive controls. The pro-inflammatory chemokines CCL2/MCP-1, CXCL9/MIG, CXCL10/IP-10, CXCL11/I-TAC or CXCL12/SDF-1α were immediately added (1 μM) to the cell-containing wells for 3 min at 37 °C. Site density per square micrometre of immobilized VCAM-1 was calculated and data are expressed as mean numbers (±s.e.m.) of adherent cells from four independent experiments.

Chemotaxis assay. The migration response of aNPCs to different chemokines was evaluated using a modified 48-well microchemotaxis Boyden chamber

system (Neuro Probe) as previously described[27]. Details are provided in the Supplementary Methods.

Apoptosis experiments. Spleen-derived $CD3^+$ cells from naive SJL mice or encephalitogenic $CD4^+$ PLP139–151-specific T-cell lines were co-cultured *in vitro* with titrated concentrations of aNPCs for 18 h at 37 °C, 7% CO_2. T cells were then harvested and FACS analysis was performed using appropriate antibodies to quantify apoptotic and necrotic $CD3^+$ cells (see Supplementary Methods for a complete list of antibodies and reagents). *In vitro* pre-treatment (30 min at 18–25 °C) of aNPCs with antibodies blocking death receptor ligands was performed using hrTRAIL-R2:Fc (10 μg ml^{-1}), mrFn14:Fc (10 μg ml^{-1}) or Fas:Fc antibodies (20 μg ml^{-1}) (all from Alexis). IFN-γ and iNOS were also blocked before performing apoptosis experiments, using either a rabbit anti-mouse IFN-γ blocking antibody (Pharmingen, 10 μg ml^{-1} for 30 min at room temperature) or by adding the iNOS inhibitor 5-methylisothiourea sulphate (Santa Cruz, 500 μM) to the co-culture wells. Data are expressed as mean percentage of positive cells over basal cells (±s.e.m.) of at least three mice per group from a minimum of three independent experiments for each protocol.

Additional experiments. The Supplementary Methods contain details regarding FACS, statistical analysis and protocols for polymerase chain reaction with reverse transcription (RT–PCR), together with lists of antibodies, cells and cell lines used.

Received 10 January; accepted 11 May 2005.

1. Lindvall, O., Kokaia, Z. & Martinez-Serrano, A. Stem cell therapy for human neurodegenerative disorders-how to make it work. *Nature Med.* **10** (suppl.), S42–S50 (2004).
2. Pluchino, S. *et al.* Injection of adult neurospheres induces recovery in a chronic model of multiple sclerosis. *Nature* **422,** 688–694 (2003).
3. McRae, B. L. *et al.* Induction of active and adoptive relapsing experimental autoimmune encephalomyelitis (EAE) using an encephalitogenic epitope of proteolipid protein. *J. Neuroimmunol.* **38,** 229–240 (1992).
4. Parras, C. M. *et al. Mash1* specifies neurons and oligodendrocytes in the postnatal brain. *EMBO J.* **23,** 4495–4505 (2004).
5. Fukuda, S. *et al.* Two distinct subpopulations of nestin-positive cells in adult mouse dentate gyrus. *J. Neurosci.* **23,** 9357–9366 (2003).
6. Lois, C., Garcia-Verdugo, J. M. & Alvarez-Buylla, A. Chain migration of neuronal precursors. *Science* **271,** 978–981 (1996).
7. Wichterle, H., Garcia-Verdugo, J. M. & Alvarez-Buylla, A. Direct evidence for homotypic, glia-independent neuronal migration. *Neuron* **18,** 779–791 (1997).
8. Alvarez-Buylla, A. & Lim, D. A. For the long run: maintaining germinal niches in the adult brain. *Neuron* **41,** 683–686 (2004).
9. Jin, K. *et al.* Vascular endothelial growth factor (VEGF) stimulates neurogenesis *in vitro* and *in vivo*. *Proc. Natl Acad. Sci. USA* **99,** 11946–11950 (2002).
10. Constantin, G. *et al.* Chemokines trigger immediate β2 integrin affinity and mobility changes: differential regulation and roles in lymphocyte arrest under flow. *Immunity* **13,** 759–769 (2000).
11. Constantin, G., Laudanna, C., Brocke, S. & Butcher, E. C. Inhibition of experimental autoimmune encephalomyelitis by a tyrosine kinase inhibitor. *J. Immunol.* **162,** 1144–1149 (1999).
12. Alt, C., Laschinger, M. & Engelhardt, B. Functional expression of the lymphoid chemokines CCL19 (ELC) and CCL 21 (SLC) at the blood–brain barrier suggests their involvement in G-protein-dependent lymphocyte recruitment into the central nervous system during experimental autoimmune encephalomyelitis. *Eur. J. Immunol.* **32,** 2133–2144 (2002).
13. Karpus, W. J. & Kennedy, K. J. MIP-1α and MCP-1 differentially regulate acute and relapsing autoimmune encephalomyelitis as well as Th1/Th2 lymphocyte differentiation. *J. Leukoc. Biol.* **62,** 681–687 (1997).
14. Furlan, R. *et al.* Intrathecal delivery of IFN-γ protects C57BL/6 mice from chronic-progressive experimental autoimmune encephalomyelitis by increasing apoptosis of central nervous system-infiltrating lymphocytes. *J. Immunol.* **167,** 1821–1829 (2001).
15. Weishaupt, A. *et al.* Molecular mechanisms of high-dose antigen therapy in experimental autoimmune encephalomyelitis: rapid induction of Th1-type cytokines and inducible nitric oxide synthase. *J. Immunol.* **165,** 7157–7163 (2000).
16. Marsden, V. S. & Strasser, A. Control of apoptosis in the immune system: Bcl-2, BH3-only proteins and more. *Annu. Rev. Immunol.* **21,** 71–105 (2003).
17. Ricci-Vitiani, L. *et al.* Absence of caspase 8 and high expression of PED protect primitive neural cells from cell death. *J. Exp. Med.* **200,** 1257–1266 (2004).
18. Schere-Levy, C. *et al.* Leukemia inhibitory factor induces apoptosis of the mammary epithelial cells and participates in mouse mammary gland involution. *Exp. Cell Res.* **282,** 35–47 (2003).
19. Tarrant, T. K. *et al.* Interleukin 12 protects from a T helper type 1-mediated autoimmune disease, experimental autoimmune uveitis, through a mechanism involving interferon gamma, nitric oxide, and apoptosis. *J. Exp. Med.* **189,** 219–230 (1999).
20. Pender, M. P. & Rist, M. J. Apoptosis of inflammatory cells in immune control of the nervous system: role of glia. *Glia* **36,** 137–144 (2001).
21. Chu, K., Kim, M., Jeong, S. W., Kim, S. U. & Yoon, B. W. Human neural stem cells can migrate, differentiate, and integrate after intravenous transplantation in adult rats with transient forebrain ischemia. *Neurosci. Lett.* **343,** 129–133 (2003).
22. Akiyama, Y. *et al.* Transplantation of clonal neural precursor cells derived from adult human brain establishes functional peripheral myelin in the rat spinal cord. *Exp. Neurol.* **167,** 27–39 (2001).
23. Vandenbark, A. A. *et al.* Differential susceptibility of human T_h1 versus T_h2 cells to induction of anergy and apoptosis by ECDI/antigen-coupled antigen-presenting cells. *Int. Immunol.* **12,** 57–66 (2000).
24. Zhang, X. *et al.* Unequal death in T helper cell (Th)1 and Th2 effectors: Th1, but not Th2, effectors undergo rapid Fas/FasL-mediated apoptosis. *J. Exp. Med.* **185,** 1837–1849 (1997).
25. Merkle, F. T., Tramontin, A. D., Garcia-Verdugo, J. M. & Alvarez-Buylla, A. Radial glia give rise to adult neural stem cells in the subventricular zone. *Proc. Natl Acad. Sci. USA* **101,** 17528–17532 (2004).
26. Constantin, G., Laudanna, C. & Butcher, E. C. Novel method for following lymphocyte traffic in mice using [^{3}H]glycerol labeling. *J. Immunol. Methods* **203,** 35–44 (1997).
27. Lazarini, F. *et al.* Differential signalling of the chemokine receptor CXCR4 by stromal cell-derived factor 1 and the HIV glycoprotein in rat neurons and astrocytes. *Eur. J. Neurosci.* **12,** 117–125 (2000).

Supplementary Information is linked to the online version of the paper at www.nature.com/nature.

Acknowledgements We wish to thank R. Galli, A. Gritti, M. Muzio, A. Vescovi and L. Ricci-Vitiani for discussions. We are grateful to F. Mavilio for critically discussing the manuscript. We acknowledge the technical help of S. Bach, S. Bucello, E. Butti, C. Covino, R. Molteni, A. Palini and C. Sciorati. S.P. is the recipient of a fellowship from the National Multiple Sclerosis Society (NMSS). L.Z. is the recipient of a fellowship from The Myelin Project (TMP). This work was supported in part by the Italian Minister of Health, the Italian Multiple Sclerosis Foundation (FISM), NMSS and TMP.

Author Information Reprints and permissions information is available at npg.nature.com/reprintsandpermissions. The authors declare no competing financial interests. Correspondence and requests for materials should be addressed to G.M. (martino.gianvito@hsr.it).